Methanogenic Activity and Microbial Community Structure in Response to Different Mineralization Pathways of Ferrihydrite in Paddy Soil

Li Zhuang[1,2], Ziyang Tang[2], Zhen Yu[2], Jian Li[2] and Jia Tang[2]*

[1] Guangdong Key Laboratory of Environmental Pollution and Health, School of Environment, Jinan University, Guangzhou, China, [2] Guangdong Key Laboratory of Agricultural Environment Pollution Integrated Control, Guangdong Institute of Eco-environmental Science & Technology, Guangzhou, China

In soils and sediments, microbial reduction of iron (hydr)oxides and consequent formation of secondary iron minerals are important factors influencing many biogeochemical cycles and processes that include microbial methanogenesis. Here, we investigated methanogenic activity and microbial community of a paddy soil enrichment in response to different biomineralization pathways of ferrihydrite, which was reduced and transformed to magnetite and vivianite in the absence and presence of phosphate, respectively. For methanogenic degradation of both acetate and propionate, CH_4 production rates in the magnetite cultures were significantly enhanced compared with the vivianite cultures. Characterization of 16S rRNA genes from methanogenic soil microbial community indicated that, (i) biomineralization of ferrihydrite was an important factor affecting soil microbial community structure; (ii) Geobacteraceae was only enriched in the vivianite cultures for both acetate- and propionate-fed incubations; and (iii) the abundance of Anaerolineaceae was increased in the magnetite cultures for both acetate- and propionate-fed incubations. The facilitated CH_4 production in the magnetite cultures might be related to the dynamic cycle of Fe(III)–Fe(II)–Fe(III) or magnetite-stimulated direct interspecies electron transfer between syntrophic acetate/propionate oxidizers and methanogens, which need further investigation. These results lend insight into the biogeochemical cycling of Fe, C, and P in anaerobic soils and sediments, as well as the development of mitigation strategies of CH_4 production.

Keywords: biomineralization of ferrihydrite, methanogenesis, phosphate, microbial community, paddy soil

INTRODUCTION

Soils and sediments contain high abundance of iron (hydr)oxides, which are important sorbents and repositories for organic and inorganic constituents (e.g., carbon tetrachloride, arsenic, and phosphate) (Cornell and Schwertmann, 2003). Thus, the dissolution and transformation of iron (hydr)oxides play important roles in controlling the fate and transport of nutrients and contaminants (Roden et al., 2002; Pedersen et al., 2006; Muehe et al., 2013a,b). Moreover, microbial reduction of iron (hydr)oxides is an important constituent of carbon and iron cycles by coupling organic matter mineralization with ferric iron reduction in anaerobic environments (Lovley, 1987;

Fredrickson and Gorby, 1996). Poorly crystalline iron (hydr)oxides are more bioavailable to dissimilatory iron-reducing bacteria (DIRB) than crystalline iron minerals as electron acceptors in anoxic soils and sediments (Lovley and Phillips, 1986; Phillips et al., 1993), thus representing a strong competitor to microbial methanogenesis (Frenzel et al., 1999; Jäeckel and Schnell, 2000; Lueders and Friedrich, 2002; Qu et al., 2004).

Poorly crystalline iron (hydr)oxides, such as ferrihydrite, are the predominate first phase of ferric-bearing minerals in soils and sediments (Tufano et al., 2009). They will transform to more stable and insoluble iron-bearing minerals due to their thermodynamic instability (Benner et al., 2002; Zachara et al., 2002; Hansel et al., 2003). In natural systems, the environmental factors controlling the formation of secondary mineralization products are complex and poorly understood (O'Loughlin et al., 2010). However, the rate and extent of Fe(II) production and its reaction with residual Fe(III) oxides and other ligands (e.g., phosphate, carbonate) are often identified as the primary controlling factors (Fredrickson et al., 1998; Dong et al., 2000; Zachara et al., 2002; Borch et al., 2007).

Depending on the geochemical conditions, ferrihydrite bioreduction leads to the formation of different secondary mineralization products including siderite (Mortimer and Coleman, 1997; Fredrickson et al., 1998), magnetite (Lovley, 1991), vivianite (Fredrickson et al., 1998), and green rust (Fredrickson et al., 1998; Parmar et al., 2001). Each secondary product has its own unique characteristics (such as crystal structure, particle size, redox potential, and conductivity), which determine its specific impact on the related biogeochemical processes. Recently, there are increasing studies investigating the association between biomineralization of iron (hydr)oxides and microbial methanogenesis (Jiang et al., 2013; Zhuang et al., 2015b; Zheng et al., 2017; Kato and Igarashi, 2019); biogenic magnetite and iron sulfides are demonstrated to enhance methanogenesis in soil and sediment. As the first attempt, our previous study (Tang et al., 2016) investigated the response of methanogenic activity to different transformation pathways of ferrihydrite in the artificial coculture of *Geobacter* and *Methanosarcina*. Methanogenic activity of the coculture is found to be associated with the type of secondary mineralization product from ferrihydrite reduction. However, the pure strains cannot fully reflect microbial ecology in natural environments.

In an attempt to investigate the response of methanogenic soil exposed to different pathways of iron biomineralization, the methanogenic activity and microbial community of a methanogenic paddy soil enrichment degrading acetate or propionate were compared under different biomineralization pathways of ferrihydrite, acting as a surrogate of bioavailable iron (hydr)oxides in soils. The different pathway of ferrihydrite biotransformation in this study was manipulated by changing the concentration of phosphate. In the presence and absence of phosphate, ferrihydrite bioreduction was expected to form mineral product of vivianite and magnetite, which further affected methanogenic activity and microbial community structure

of the paddy soil enrichment. Results from this study might provide an enhanced understanding of microorganisms involved in biogeochemical cycling of carbon and iron in natural environments.

EXPERIMENTAL METHODS

Anaerobic Incubation Experiments

The soil used in this experiment was sampled from the 0- to 20-cm layers in a rice paddy field located at the South China Botanical Garden. The physiochemical properties of the soil sample were determined (Zhuang et al., 2015b), and the results included pH (6.4), organic matters (26.9 g/kg), total Fe (19.5 g/kg), NO_3^- (0.92 g/kg), SO_4^{2-} (1.2 g/kg), total phosphorus (0.63 g/kg), and total nitrogen (2.3 g/kg). Before anaerobic incubation, the soil samples were immersed in deionized water for 1 month to remove the presence of electron acceptors, such as Fe(III), nitrate, and sulfate, then air-dried and sieved (<74 µm). All of the anaerobic incubations were carried out in 275-ml serum bottles, each containing 50 ml of anaerobic medium, 0.5 g of dry soil, 30 mM ferrihydrite (if required), and 5.0 mM acetate or 3.0 mM propionate as a methanogenic substrate. The details for treatments were described in **Supplementary Table S1**.

Prepared as previously described with slight modifications (Kato et al., 2012), the anaerobic medium consisted of 10 mM NH_4Cl, 0.5 mM $MgCl_2$, 0.5 mM $CaCl_2$, 5 mM $NaHCO_3$, 10 mM 4-(2-hydroxyethyl)-1-piperazineethanesulfonic acid (HEPES), and 1 ml L^{-1} each of a trace element solution and Se/W solution. The composition of the trace element solution are nitrilotriacetic acid (12.8 g/L), $FeCl_3 \cdot 6H_2O$ (1.35 g/L), $MnCl_2 \cdot 4H_2O$ (0.1 g/L), $CoCl_2 \cdot 6H_2O$ (0.024 g/L), $CaCl_2 \cdot 2H_2O$ (0.1 g/L), $ZnCl_2$ (0.1 g/L), $CuCl_2 \cdot 2H_2O$ (0.025 g/L), H_3BO_3 (0.01 g/L), $Na_2MoO_4 \cdot 2H_2O$ (0.024 g/L), NaCl (1.0 g/L), and $NiCl_2 \cdot 6H_2O$ (0.12 g/L). The Se/W solution consists of $Na_2SeO_3 \cdot 5H_2O$ (0.026 g/L) and $Na_2WO_4 \cdot H_2O$ (0.003 g/L).

The different biomineralization pathways of ferrihydrite were regulated by the presence or absence of phosphate. One treatment was conducted with phosphate-free PSN medium, and the other was conducted using anaerobic medium containing 4.0 mM phosphate. The stock solution of ferrihydrite was synthesized by neutralizing 0.4 M ferric chloride solution with 1 M NaOH to a pH of approximately 7.0 (Schwertmann and Cornell, 2000). All of the bottles were sealed with Teflon®-coated septa and aluminum crimp caps after being bubbled with $N_2:CO_2$ [(80: 20) v/v] gas at a rate of 10 ml min^{-1} for 1 h. Four feeding cycles were carried out for acetate-fed enrichments, and each dose was approximately 4.7–5.1 mM. Three feeding cycles were conducted for propionate-fed enrichments, and each dose was approximately 2.7–3.0 mM. A new feeding cycle was initiated as acetate or propionate was reapplied after its complete depletion in the previous cycle. The incubation period timelines for each treatment were presented in **Supplementary Table S2**. All of the experiments were conducted in biological triplicates and incubated at 30°C at a constant temperature incubator without agitation in the dark.

Chemical Analysis

The concentrations of CH_4 were determined using a GC7900 gas chromatograph (TECHCOMP Instruments, Shanghai, China) equipped with a flame ionization detector (FID). The temperatures of the inlet, the oven, and the detector were 120, 80, and 170°C, respectively. The injection volume was 200 μl, and the minimum detection limit of CH_4 was 2 ppmv. The gas in the headspace was taken using a gas-tight syringe (Hamilton, Switzerland). Gas sampling was conducted every 3–5 days in the early phase and every 1–2 days in the middle and later stages of the experiment. The concentrations of propionate and acetate were determined with HPLC (Shimadzu) using an SPD-15C column (150 mm × 4.6 mm; 5 μm pore size), and the lower detection limit was 1 mg L^{-1}. The HCl-extractable Fe(II) concentrations were determined via the ferrozine technique, as described previously (Lovley and Phillips, 1986).

X-ray diffraction (XRD) analysis was used to identify the species of secondary mineralization products. Considering that the silicate and clay mineral in soil samples interfere with the spectrum of iron minerals, the identification of secondary minerals from ferrihydrite bioreduction was conducted in the anaerobic incubations inoculated with the bacterial suspension free from soil particles, which was prepared by incubating paddy soil in PSN medium.

Before XRD analyses, the samples were centrifuged at 4,000 rpm for 5 min, washed twice with deionized water (5 min each time), and then dried overnight in a vacuum desiccator. All of the XRD analyses were performed with a PANalytical (Netherlands) X'pert Pro MPD (at 40 kV and 40 mA) using CuK$_{\alpha\ 1,2}$ radiation (0.15406 and 0.15444 nm), with a scan rate of 0.1°θ/min.

Microbial Community Analysis

The soil enrichments at the end of the incubation period (when CH_4 production approached a plateau in the last feeding cycle) and the initial soil were subjected to DNA extraction, 16S rRNA gene amplification, and 16S rRNA sequencing for microbial community analysis. DNA was extracted using a PowerSoil^{TM} DNA isolation kit (MO BIO Laboratories, United States) according to the manufacturer's instructions. The primer set 515F (GTGCCAGCMGCCGCGGTAA) and 806R (GGACTACHVGGGTWTCTAAT) was used for amplifying the V4 hypervariable regions of the bacterial and archaeal 16S rRNA genes. A 30-μl PCR mixture contained 0.75 units Ex Taq DNA polymerase (TaKaRa, Dalian, China), 1 × Ex Taq loading buffer (TaKaRa, Dalian, China), 0.2 mM dNTP mix (TaKaRa, Dalian, China), 0.2 μM each primer, and 100 ng template DNA. The amplification conditions used were as follows: an initial denaturation temperature of 94°C for 5 min; 35 cycles of 94°C for 30 s; 53°C for 60 s and 72°C for 60 s; and a final elongation step at 72°C for 7 min. The amplicons were sequenced on an Illumina MiSeq platform by Novogene Bioinformatics Technology (Beijing, China).

Pairs of reads from the original DNA fragments were merged by using FLASH (Magoč and Salzberg, 2011) after low-quality reads were removed by Perl scripts. Then, sequences were analyzed with the QIIME software package (Caporaso et al., 2010) and the UPARSE pipeline (Edgar, 2013) with default parameters. Operational taxonomic units (OTUs) were defined at the sequence similarity level of 97%, and a representative sequence from each OTU was assigned to a taxonomic identity using Ribosomal Database Project (RDP) classifier (version 2.2) with a default confidence threshold of 0.8–1.0. Principal coordinates analysis (PCoA) was conducted based on the Bray-Curtis distance. To visualize the microbial communities, we constructed a heat map by applying the heatmap.2 function implemented in the gplots R package. Most dominant phyla (at the family level) with a maximum abundance of more than 1% in all samples were included in the heat map. The raw sequence data have been deposited in the sequence read archive of NCBI with the following accession number: SRR565746.

Statistical Analysis

Significant differences among treatments were tested by the ANOVA method using the SPSS software package (SPSS Inc., 2003). Differences between values were considered to be statistically significant at $P < 0.05$.

RESULTS

Different Mineralization Pathways of Ferrihydrite

Here, we manipulated the different secondary mineralization pathways induced by the bioreduction of ferrihydrite with and without the addition of phosphate in the soil enrichments. After an incubation period of 18 days, in the phosphate-free acetate-fed incubations, the reddish brown ferrihydrite was changed to black solids that can strongly be attracted by magnets, whereas the secondary minerals from ferrihydrite bioreduction in the presence of phosphate did not possess magnetic characteristics. The ultimate iron minerals were characterized using XRD. The iron particles in the phosphate-free incubations were identified as magnetite by the characteristic diffraction pattern of lines 311, 400, 422, 511, and 440 in XRD measurements (**Supplementary Figure S1A**), and the presence of phosphate resulted in the formation of vivianite as the secondary mineralization product (**Supplementary Figure S1B**). With a longer incubation period (40 days) in the propionate-fed incubations, the transformation of ferrihydrite occurred *via* similar pathways resulting in the predominant production of magnetite and vivianite in the absence and presence of phosphate, respectively (**Supplementary Figure S2**).

Regardless of the presence of phosphate, ferrihydrite reduction coupled with acetate/propionate degradation resulted in similar Fe(II) generation and accumulation in both soil enrichments (**Supplementary Figures S3, S4**). In the acetate-fed incubations, the total HCl-extractable Fe(II) production accumulated to the maximum values of 19.6 and 16.7 mM on day 6 in the cultures with and without phosphate, respectively (**Supplementary Figure S3A**). From day 12 on, Fe(II) concentrations were stabilized approximately 13 mM, and acetate was further degraded *via* methanogenesis (**Supplementary Figure S3B**).
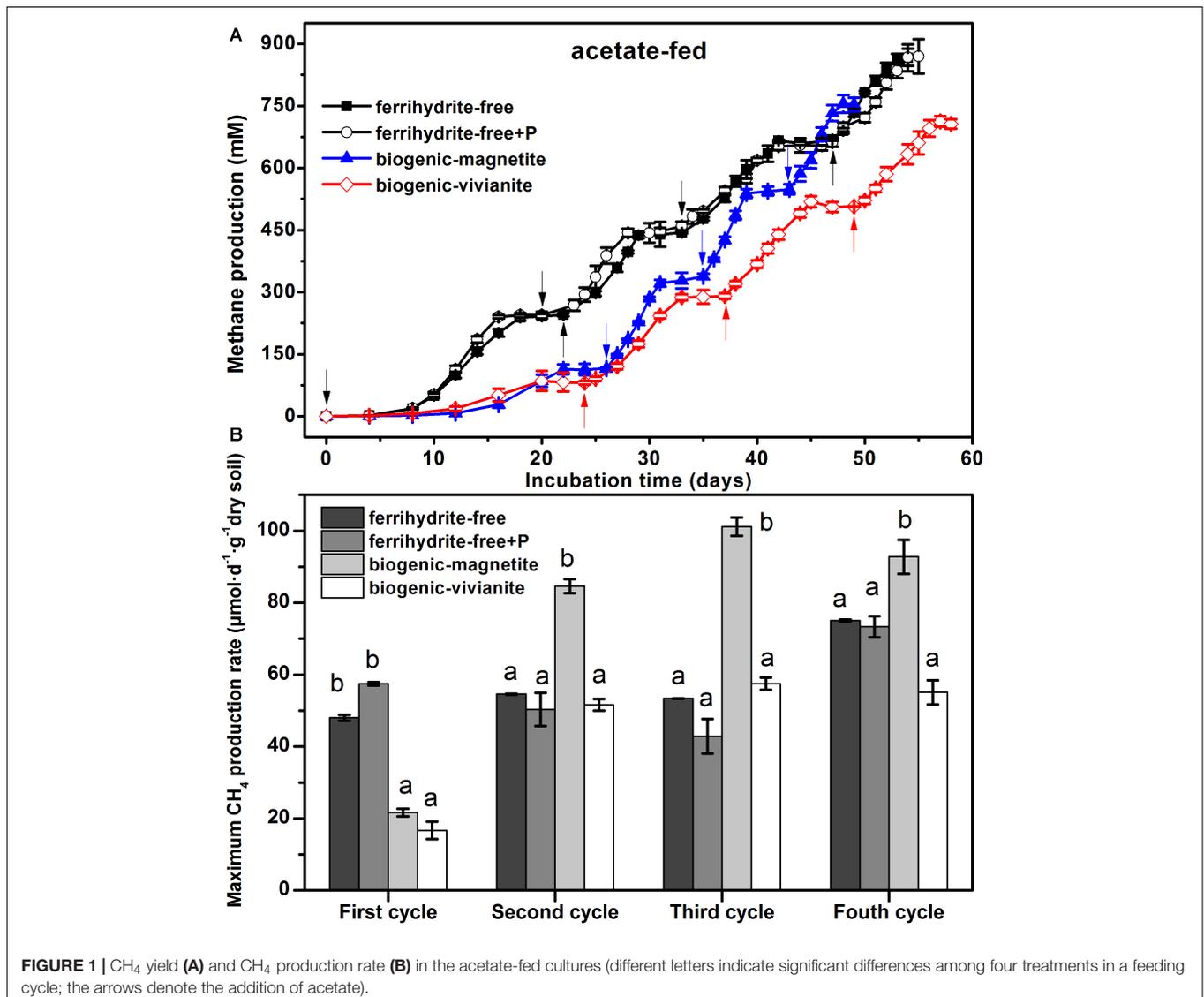
For the propionate-fed incubations, the total HCl-extractable Fe(II) production accumulated to the maximum values of 16.8 and 15.5 mM on day 10 in the cultures with and without phosphate, respectively. Fe(II) concentrations were maintained in the range of 12–14 mM during the subsequent incubation time (**Supplementary Figure S4A**). Acetate was produced as an intermediate during ferrihydrite reduction coupling with propionate degradation (**Supplementary Figure S4B**).

Methanogenesis From Acetate in Response to Different Mineralization Pathways of Ferrihydrite

For a concise description, in the following sections, "BM-cultures" and "BV-cultures" are used to denote anaerobic incubations with the biogenic formation of magnetite and vivianite as a consequence of biomineralization of ferrihydrite in the absence and presence of phosphate, respectively.

"FF-cultures" and "FFP-cultures" are used to denote the anaerobic incubations without ferrihydrite in the absence and presence of phosphate, respectively.

The conversion of acetate to CH_4 in all incubations was compared in terms of CH_4 cumulative yield (**Figure 1A**) and maximum CH_4 production rates (**Figure 1B**). Data showed that CH_4 production patterns were rather similar in the ferrihydrite-free cultures (FF- and FFP-cultures), regardless of the presence of phosphate, and approached the maximum CH_4 production of 865 ± 32 and 870 ± 41 μmol at the end of the incubation. In the first feeding cycle, methanogenesis in both BM- and BV-cultures was suppressed by the bioreduction of ferrihydrite. In the second to fourth feeding cylces, 94–102% of the electrons expected from acetate oxidation were recovered as CH_4 (**Supplementary Table S3**) according to stoichiometric conversion of acetate to CH_4 ($CH_3COO^- + H^+ \rightarrow CH_4 + CO_2$). The BM- and BV-cultures accumulated a total CH_4 production of 755 ± 21 and 712 ± 12 μmol, respectively, at the end of incubation.

FIGURE 1 | CH_4 yield **(A)** and CH_4 production rate **(B)** in the acetate-fed cultures (different letters indicate significant differences among four treatments in a feeding cycle; the arrows denote the addition of acetate).
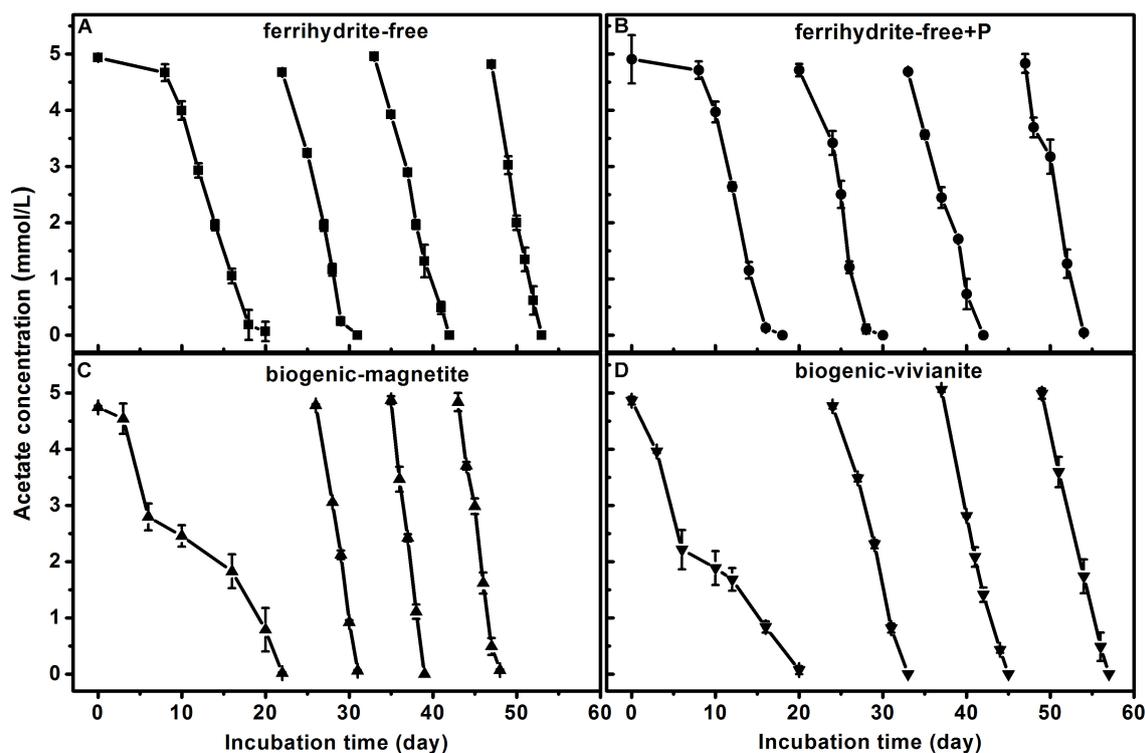
FIGURE 2 | Acetate degradation in different treatments: **(A)** ferrihydrite-free cultures, **(B)** ferrihydrite-free + P cultures, **(C)** biogenic-magnetite cultures, and **(D)** biogenic-vivianite cultures (the arrows denote the addition of acetate).
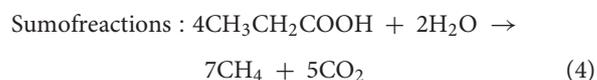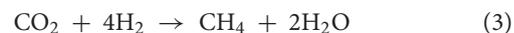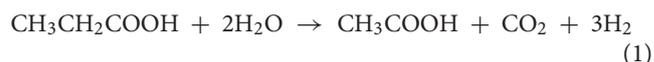
In the first feeding cycle, the BM- and BV-cultures produced CH_4 with a much lower rate than that in the ferrihydrite-free cultures due to the competition for acetate between methanogens and Fe(III)-reducing bacteria. In the second to fourth feeding cycles, the maximum CH_4 production rates in the BM-cultures were 84.6 ± 1.97, 101.2 ± 2.56, and 92.8 ± 4.72 μmol day^{-1} g^{-1} dry soil, which were significantly greater than those in the FF-, FFP-, and BV-cultures (specific rates for each cycle are summarized in **Supplementary Table S4**). The kinetics of acetate degradation corresponded to the kinetics of CH_4 production, and a higher acetate degradation rate corresponded to a higher CH_4 production rate (**Figure 2**).
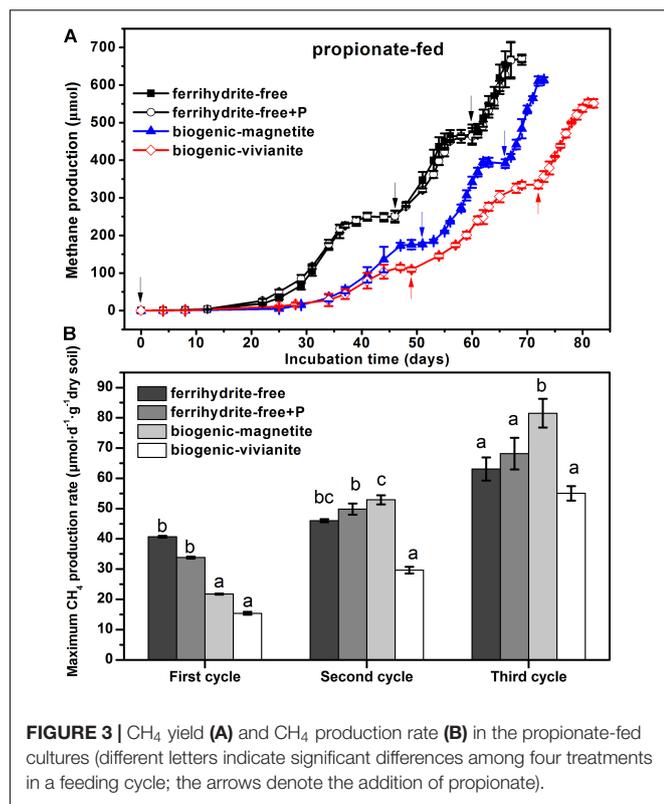
Methanogenesis From Propionate in Response to Different Mineralization Pathways of Ferrihydrite

Compared with the lag phase of acetate degradation to CH_4 (8 days), the conversion of propionate to CH_4 was initiated after a longer lag phase (25 days). The patterns of CH_4 cumulative yield (**Figure 3A**) and maximum production rates (**Figure 3B**) in the propionate-fed cultures were very similar to those of the acetate-fed cultures. It is noted that CH_4 production rates increased with the feeding cycles for all of the incubations. The maximum CH_4 production rates in the BM-cultures derived from the three cycles were 21.7 ± 0.17,

52.9 ± 1.5, and 81.5 ± 4.7 μmol day^{-1} g^{-1} dry soil, which were 41, 79, and 48% greater than those in the BV-cultures, respectively.

The faster propionate degradation rates corresponded to the higher CH_4 production rates (**Figure 4**). As propionate was degraded, the concentration of acetate followed a pattern of steady increase to a peak and subsequent decrease, suggesting that acetate was an intermediate metabolite in propionate degradation to CH_4. The maximum acetate concentrations were observed to be 1.4, 1.3, 1.0, and 1.1 mmol·L^{-1} in the FF-, FFP-, BM-, and BV-cultures, respectively. Each mole of propionate yielded 1.57–1.78 mol of CH_4, which was close to the theoretic stoichiometry of the complete degradation of propionate to CH_4 (Eqs 1–4, 1 mol propionate yields 1.75 mol CH_4). Acetate produced from propionate oxidation (Eq. 1) was further converted to CH_4 by methanogens.

$$CH_3CH_2COOH + 2H_2O \rightarrow CH_3COOH + CO_2 + 3H_2 \tag{1}$$

$$CH_3COOH \rightarrow CH_4 + CO_2 \tag{2}$$

$$CO_2 + 4H_2 \rightarrow CH_4 + 2H_2O \tag{3}$$

$$\text{Sumofreactions}: 4CH_3CH_2COOH + 2H_2O \rightarrow$$
$$7CH_4 + 5CO_2 \tag{4}$$

FIGURE 3 | CH_4 yield **(A)** and CH_4 production rate **(B)** in the propionate-fed cultures (different letters indicate significant differences among four treatments in a feeding cycle; the arrows denote the addition of propionate).

Based on the stoichiometry from Eq. 4, it was calculated that CH_4 production accounted for 90–102% of the electrons expected from propionate oxidation in each feeding cycle (**Supplementary Table S5**), suggesting that methanogenesis was the sole electron-accepting process for metabolism.

Microbial Community Analysis of the Acetate-Fed Incubations

From DNA samples in the acetate-fed incubations, we obtained an average of $62,787 \pm 10,214$ high-quality 16S rRNA gene sequence reads, and the sequences were clustered into $2,914 \pm 488$ OTUs per sample. **Figure 5** displayed the microbial community clustering using PCoA-weighted UniFrac distances. Samples from the ferrihydrite-free incubations (FF and FFP) were separated by principle component 1; samples from the incubations suffering ferrihydrite bioreduction (BM and BV) were closely clustered.

The relative abundances of OTUs at the phylum level in the initial soils and acetate-fed cultures are described in **Supplementary Figure S5**. The most predominant phyla of bacteria identified in all of the incubations belonged to *Proteobacteria* (26.5–43.2%), Firmicutes (12.6–18.9%), Chloroflexi (9.0–18.7%), and Bacteroidetes (4.8–14.6%). Compared with the initial soil sample (0.5%), methanogenic degradation of acetate enriched the relative abundance of Euryarchaeota in the acetate-fed cultures (1.3–13.3%). To further investigate the key microorganisms involved in methanogenesis from acetate, we plotted a heat map showing the shift in relative

abundance of the most abundant bacterial and archaeal taxa at the family level in all of the samples (**Figure 6**). Relative to the initial soil samples (D0), the bacterial family Pseudomonadaceae was enriched in all of the acetate-fed cultures at the end of incubation. Compared with the ferrihydrite-free cultures (FF and FFP), acetate conversion to CH_4 in the presence of ferrihydrite bioreduction (BM and BV) enriched the relative abundance of the families Anaerolinaceae, Clostridiaceae, Peptococcaceae, Myxococcaceae, and Syntrophaceae, and the extents of enrichment in the BM-cultures were greater than those in the BV-cultures. The relative abundance of Syntrophomonadaceae was also increased, but members of this family are not known to be capable of oxidizing acetate (Sobieraj and Boone, 2006). In terms of methanogens, Methanocellaceae abundance was highly enriched in the ferrihydrite-free incubations (FF and FFP), while Methanosarcinaceae abundance in the FFP-cultures was highest.

Microbial Community Analysis of the Propionate-Fed Incubations

From DNA samples in the propionate-fed incubations, we obtained an average of $65,818 \pm 5,647$ high-quality 16S rRNA gene sequence reads, and the sequences were clustered into $2,836 \pm 460$ OTUs per sample. PCoA plot (**Figure 7**) indicated that principle component 1 clearly separated the propionate-fed incubations from the initial soil samples, whereas principle component 2 separated the ferrihydrite-free (FF and FFP) and ferrihydrite bioreduction incubations (BM and BV).

The relative abundances of OTUs at the phylum level in the initial soil and propionate-fed cultures are described in **Supplementary Figure S6**. The major bacterial populations belonged to the phyla *Proteobacteria* (22.0–36.4%), Firmicutes (12.9–24.1%), and Chloroflexi (9.6–21.3%). Compared with the initial soil sample (0.5%), methanogenic degradation of propionate increased the relative abundance of Euryarchaeota in the propionate-fed cultures (2.5–20.9%). As shown in **Figure 8**, relative to the initial soil samples, the families of Syntrophaceae and Desulfovibrionaceae were enriched in all the propionate-fed cultures at the end of incubation. The increase in Syntrophomonadaceae was not of a concern here because they are irrelevant in their utilization of propionate (Sobieraj and Boone, 2006). Methanogenic propionate degradation in the presence of ferrihydrite bioreduction (BM and BV) enriched the relative abundances of the bacterial families Desulfobacteraceae, Desulfovibrionaceae, and Syntrophobacteraceae and the archaeal families Methanosarcinaceae and Methanocellaceae. The microbial community characteristics of the BM- and BV-cultures are distinct: Methanocellaceae, Methanosarcinaceae, and Anaerolineaceae were highly enriched in the BM-cultures, whereas Methanosarcinaceae, Gracilibacteraceae, Peptococcaceae, Geobacteraceae, and Myxococcaceae were significantly increased in the BV-cultures.

DISCUSSION

Phosphate is an important nutrient element for microbial growth and an environmental factor influencing the bioreduction
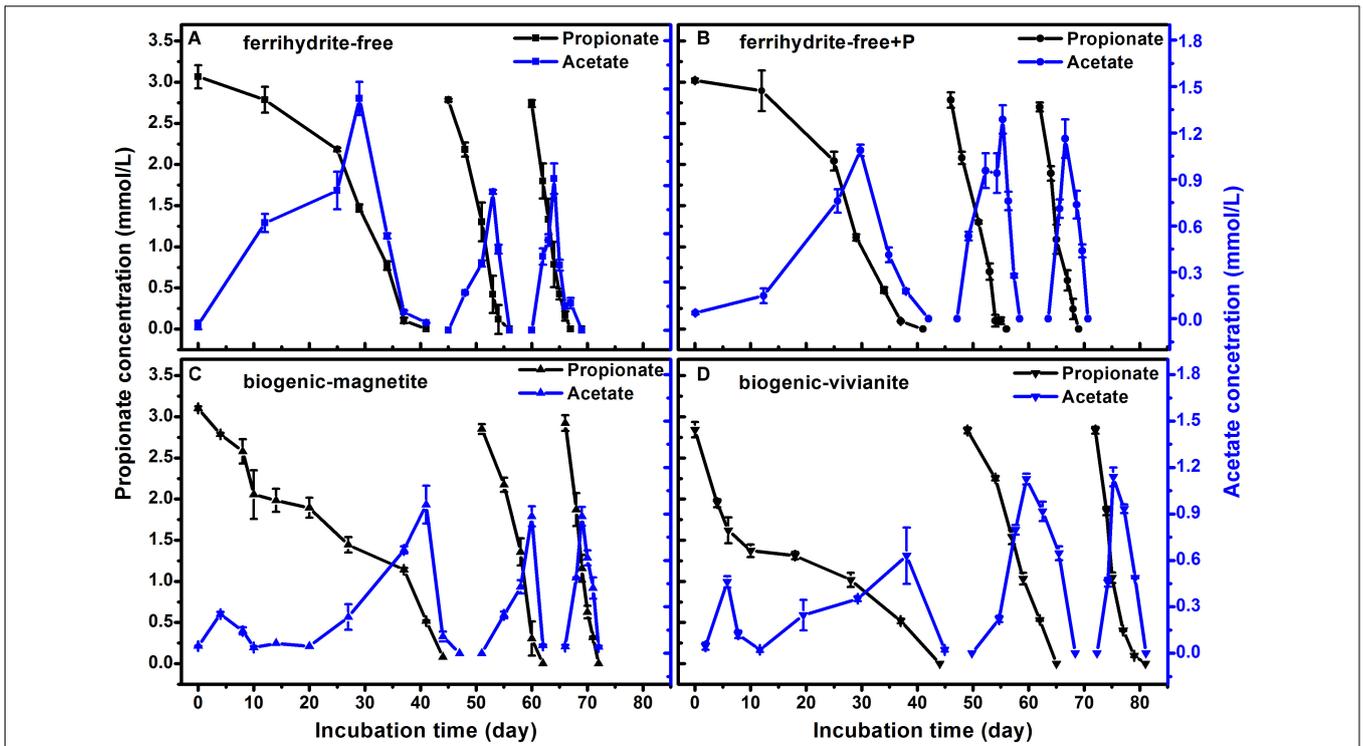
FIGURE 4 | Propionate degradation and the appearance and disappearance of acetate in different treatments: **(A)** ferrihydrite-free cultures, **(B)** ferrihydrite-free + P cultures, **(C)** biogenic-magnetite cultures, and **(D)** biogenic-vivianite cultures (the arrows denote the addition of propionate).
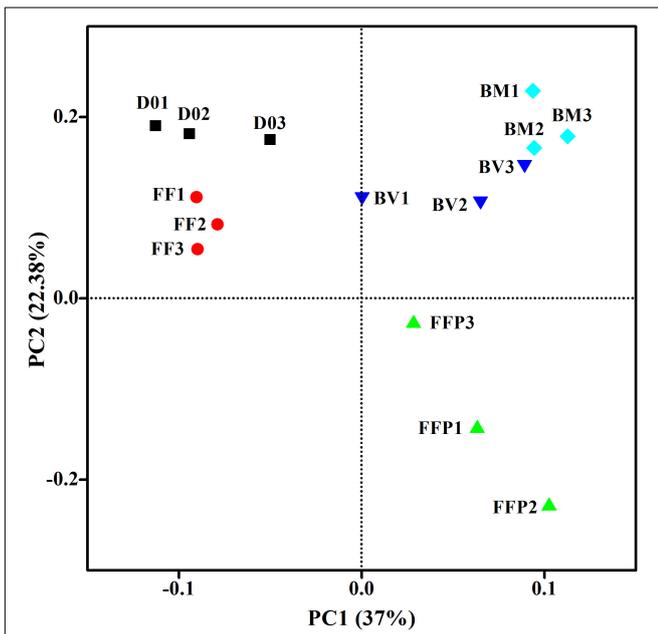

FIGURE 5 | Principal coordinates analysis (PCoA) of microbial communities in initial soil samples and acetate-fed samples based on the weighed UniFrac distance (D01–D03: triplicates of initial soil sample; FF1–FF3: triplicates of ferrihydrite-free cultures; FFP1–FFP3: triplicates of ferrihydrite-free + P cultures; BM1–BM3: triplicates of biogenic-magnetite cultures; and BV1–BV3: triplicates of biogenic-vivianite cultures).
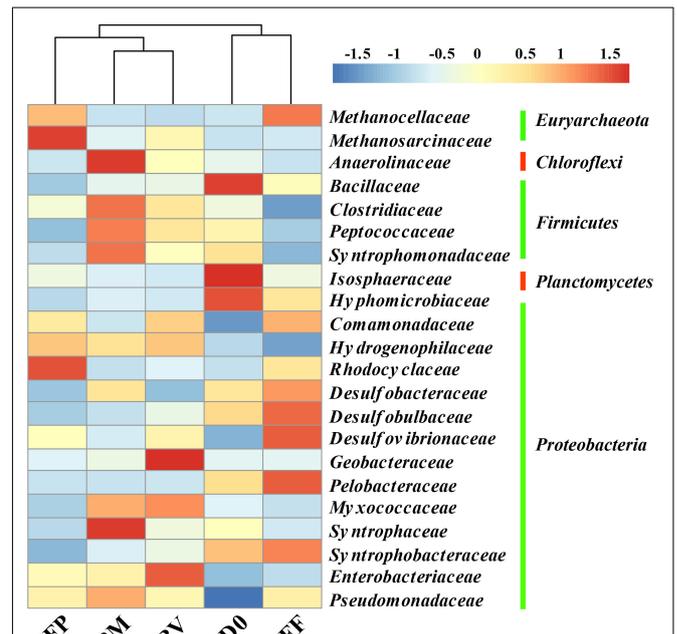

FIGURE 6 | Heat map of the relative abundance of the most abundant operational taxonomic units (OTUs) (the abundance >2%) from initial soil samples and acetate-fed samples (D0: initial soil sample; FF: ferrihydrite-free cultures; FFP: ferrihydrite-free + P cultures; BM: biogenic-magnetite cultures; and BV: biogenic-vivianite cultures).
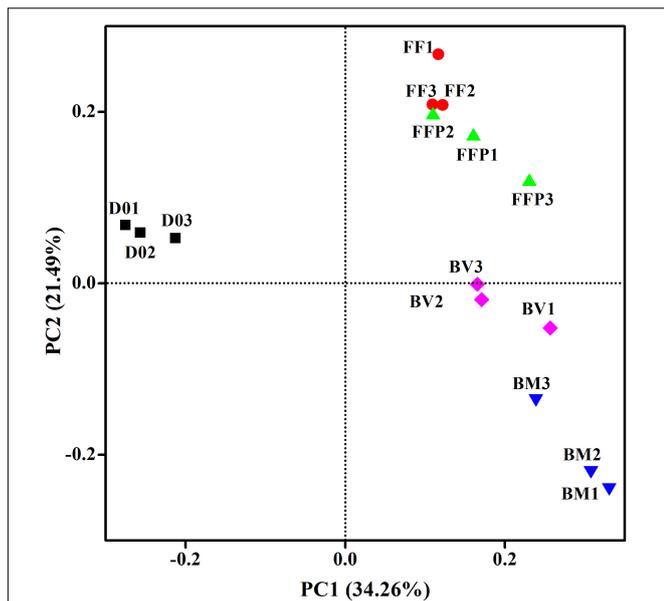
FIGURE 7 | Principal coordinates analysis (PCoA) of microbial communities in initial soil samples and propionate-fed samples based on the weighed UniFrac distance (D01-D03: triplicates of initial soil sample; FF1–FF3: triplicates of ferrihydrite-free cultures; FFP1–FFP3: triplicates of ferrihydrite-free + P cultures; BM1–BM3: triplicates of biogenic-magnetite cultures; and BV1–BV3: triplicates of biogenic-vivianite cultures).
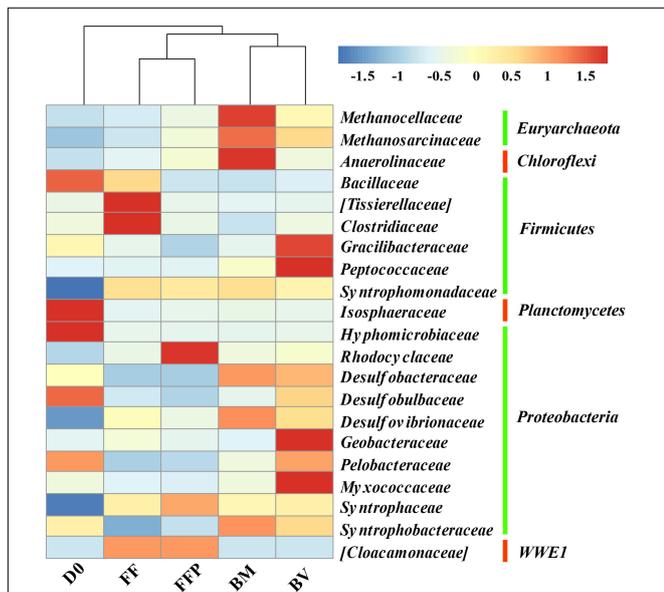

FIGURE 8 | Heat map of the relative abundance of the most abundant operational taxonomic units (OTUs) (the abundance >1%) from initial soil samples and propionate-fed samples (D0: initial soil sample; FF: ferrihydrite-free cultures; FFP: ferrihydrite-free + P cultures; BM: biogenic-magnetite cultures; and BV: biogenic-vivianite cultures).

and mineralization pathway of iron (hydr)oxides, acting as sorbing oxyanions to change the surface reactivity of iron (hydr)oxides (Borch et al., 2007). In the present study,

due to the strong surface complexation of phosphate with ferrihydrite, the presence of phosphate promoted the formation of vivianite. Magnetite was the most appreciable mineralization product in the absence of phosphate in this study, which was consistent with previous studies (Kukkadapu et al., 2004; Tang et al., 2016). Without ferrihydrite bioreduction in the paddy soil enrichments, phosphate exerted very slight effects on methanogenic degradation of acetate and propionate, however, by means of changing the biomineralization pathway of ferrihydrite, the addition of phosphate significantly influenced methanogenic processes. This finding might cast a new light on the biogeochemical cycling of C, Fe, and P in anoxic soils and sediments.

PCoA (**Figures 5**, **7**) revealed that, in the absence of ferrihydrite reduction, phosphate was an important factor affecting communities in the acetate-fed incubations but was not the case for the propionate-fed incubations. For both acetate- and propionate-fed incubations, the BM- and BV-cultures were always clustered together and distinct from the other samples, which suggest that biomineralization of ferrihydrite is an important contributor to microbial community structural changes.

Geobacteraceae, the representative dissimilatory Fe(III)-reducing bacteria responsible for microbial Fe(III) reduction in paddy soils (Hori et al., 2010; Yi et al., 2013), was only enriched in the BV-cultures for both cases of feeding with acetate and propionate. The low abundance of Geobacteraceae in the BM-cultures might be related to the low level of phosphate during ferrihydrite reduction because phosphate availability has been reported to limit the growth of *Geobacter* species (N'Guessan et al., 2010). The communities of *Clostridium* have been demonstrated to be closely correlated with microbial Fe(III) reduction (Li et al., 2017), and some species of family Peptococcaceae are iron reducers (Kunapuli et al., 2007; Burkhardt et al., 2010). Thus, the enrichment of Peptococcaceae and Clostridiaceae in the BM-cultures might have resulted from ferrihydrite bioreduction with acetate. As a metal-reducing family, the relative abundance of Desulfovibrionaceae (Tebo and Obraztsova, 1998) was increased in the BM-cultures fed with propionate and might play an important role during Fe(III) reduction coupling with propionate oxidization.

For all of the incubations, Methanocellaceae and Methanosarcinaceae are the predominant methanogens. All of the species in the Methanocellaceae family are found in rice field soils (Sakai et al., 2008, 2010; Lü and Lu, 2012), and many of them are the dominant methanogens in the paddy soil cultured with acetate (Rui et al., 2011). They produce CH_4 from H_2/CO_2 or formate, and acetate is required as a carbon source for growth. The family Methanosarcinaceae is the most versatile of all families of methanogenic archaea with respect to the diversity of substrates used for CH_4 generation (Oren, 2014). Recently, *Methanosarcina barkeri* has been reported to be capable of conserving energy from CO_2 reduction to CH_4 with the electrons received via direct interspecies electron transfer (DIET) (Rotaru et al., 2014). In the present study, both the biomineralization of ferrihydrite and the presence of phosphate affected the relative abundances of Methanocellaceae

and Methanosarcinaceae in both acetate- and propionate-fed incubations (**Figures 6**, **8**).

In the case of acetate, Anaerolinaceae, Clostridiaceae, Peptococcaceae, and Syntrophaceae were enriched in the BM-cultures compared with the BV-cultures. Although most Clostridiaceae species are fermenting bacteria, Jiang et al. (2013) reported a syntrophic interaction between *Clostridium* and *Methanosarcina* converting acetate to CH_4 during the biotransformation of akaganeite to goethite. Compared with the BM-cultures, Desulfovibrionaceae, Geobacteraceae, and *Enterobacteriaceae* increased in the BV-cultures. *Geobacter* spp. are capable of establishing syntrophic interactions with methanogenic archaea in the presence of acetate, and methanogenesis can be facilitated by conductive minerals (Kato et al., 2012; Yamada et al., 2015; Zhuang et al., 2015b; Tang et al., 2016). This implied that different microorganisms might be involved in CH_4 production by syntrophic acetate oxidation in the BM- and BV-cultures. In the case of propionate, the bacterial families Anaerolineaceae, Desulfovibrionaceae, and Syntrophobacteraceae were enriched the BM-cultures. Of them, Syntrophobacteraceae is capable of converting propionate to acetate and syntrophically interacting with H_2- and formate-utilizing methanogens (Boone and Bryant, 1980; Kuever, 2014; Liu and Conrad, 2017). In the BV-cultures, the relative abundances of Gracilibacteraceae, Peptococcaceae, Geobacteraceae, and Myxococcaceae were highly increased. This finding suggested that the syntrophic propionate-oxidizing communities were changed by biomineralization of ferrihydrite.

It is noted that the family Anaerolineaceae was highly enriched in the BM-cultures fed with either acetate or propionate. Anaerolineaceae species have been demonstrated to be the most predominant bacteria in alkanes-dependent methanogenic culture (Liang et al., 2015). Members of the class Anaerolineae have a filamentous morphology, which may facilitate their cooperation with other microorganisms (Sekiguchi et al., 2001; Yamada et al., 2005), such as methanogens. On the other hand, Anaerolineae have been found as the predominant populations on the anodes of microbial fuel cell inoculated with soil, especially with rice field soils (Ishii et al., 2008; Cabezas et al., 2015), and thus they might possess the capability of extracellular electron transfer. Thus, Anaerolineae might have the ability to provide electrons directly to other microorganisms, likely Methanosarcinaceae species that are capable of accepting electrons via DIET (Rotaru et al., 2014).

Interestingly, the biotransformation of ferrihydrite to magnetite (BM-cultures) facilitated CH_4 production from both acetate and propionate in the present study. There are two potential explanations: (i) the dynamic iron cycling of Fe(III)(ferrihydrite)–Fe(II)(liquid)–Fe(III)(magnetite) might accelerate the electron flow from acetate/propionate oxidation to hydrogenotrophic methanogenesis, similar to that proposed by Jiang et al. (2013). In their hypothesis, syntrophic acetate oxidizing bacteria reduced akaganeite to release Fe(II), which was readsorbed and reprecipitated as structural Fe(III) with goethite formation. Methanogens harnessed electrons from Fe(II) for CO_2 reduction to CH_4, which accelerated CH_4

production from acetate. (ii) Conductive magnetite served as a conduit for DIET between syntrophic acetate/propionate oxidizers and methanogens possibly between Anaerolineaceae and Methanosarcinaceae. Many studies have demonstrated that the presence of magnetite nanoparticles can accelerate syntrophic methanogenesis by stimulating DIET (Kato et al., 2012; Viggi et al., 2014; Li et al., 2015; Yamada et al., 2015; Zhuang et al., 2015a). It would be interesting to further investigate DIET-mediated methanogenesis in our experimental system, especially the DIET function of Anaerolineaceae.

CONCLUSION

In this study, different mineralization pathways of ferrihydrite in paddy soil enrichments were regulated by the concentration of phosphate. Experimental results indicated that both methanogenic activities and microbial community structure during the conversion of acetate/propionate to CH_4 were affected by the biomineralization of ferrihydrite. When magnetite was formed as the predominant secondary iron minerals, methanogenesis from acetate and propionate was facilitated relative to those incubations with vivianite formation from ferrihydrite reduction. The accelerated CH_4 production from acetate and propionate in the magnetite cultures might be related to the Fe(III)–Fe(II)–Fe(III) cycle or magnetite-facilitated DIET and needs further investigation.

DATA AVAILABILITY STATEMENT

The datasets generated for this study can be found in NCBI, SRR5657646.

AUTHOR CONTRIBUTIONS

LZ and JT designed the research and wrote the initial manuscript. JL, ZT, and JT developed the methodology and generated the data. LZ and ZY performed the statistical analysis. LZ and JT contributed to the final manuscript.

FUNDING

SUPPLEMENTARY MATERIAL

The Supplementary Material for this article can be found online at: https://www.frontiersin.org/articles/10.3389/feart.2019.00325/full#supplementary-material

REFERENCES

Benner, S., Hansel, C., Wielinga, B., Barber, T., and Fendorf, S. (2002). Reductive dissolution and biomineralization of iron hydroxide under dynamic flow conditions. *Environ. Sci. Technol.* 36, 1705–1711. doi: 10.1021/es0156441

Boone, D. R., and Bryant, M. P. (1980). Propionate-degrading bacterium, *Syntrophobacter wolinii* sp. nov. gen. nov. from methanogenic ecosystems. *Appl. Environ. Microbiol.* 40:626.

Borch, T., Masue, Y., Kukkadapu, R. K., and Fendorf, S. (2007). Phosphate imposed limitations on biological reduction and alteration of ferrihydrite. *Environ. Sci. Technol.* 41, 166–172. doi: 10.1021/es060695p

Burkhardt, E. M., Akob, D. M., Bischoff, S., Sitte, J., Kostka, J. E., Banerjee, D., et al. (2010). Impact of biostimulated redox processes on metal dynamics in an iron-rich creek soil of a former uranium mining area. *Environ. Sci. Technol.* 44, 177–183. doi: 10.1021/es902038e

Cabezas, A., Pommerenke, B., Boon, N., and Friedrich, M. W. (2015). *Geobacter*, *Anaeromyxobacter* and *Anaerolineae* populations are enriched on anodes of root exudate-driven microbial fuel cells in rice field soil. *Environ. Microbiol. Rep.* 7, 489–497. doi: 10.1111/1758-2229.12277

Caporaso, J. G., Kuczynski, J., Stombaugh, J., Bittinger, K., Bushman, F. D., and Costello, E. K. (2010). QIIME allows analysis of high-throughput community sequencing data. *Nat. Methods* 7, 335–336. doi: 10.1038/nmeth.f.303

Cornell, R. M., and Schwertmann, U. (2003). *The Iron Oxides*. New York, NY: Wiley-VCH.

Dong, H., Fredrickson, J. K., Kennedy, D. W., Zachara, J. M., Kukkadapu, R. K., and Onstott, T. C. (2000). Mineral transformation associated with the microbial reduction of magnetite. *Chem. Geol.* 169, 299–318. doi: 10.1016/S0009-2541(00)00210-2

Edgar, R. C. (2013). UPARSE: highly accurate OTU sequences from microbial amplicon reads. *Nat. Methods* 10, 996–998. doi: 10.1038/nmeth.2604

Fredrickson, J. K., and Gorby, Y. A. (1996). Environmental processes mediated by iron-reducing bacteria. *Curr. Opin. Biotech.* 7, 287–294. doi: 10.1016/S0958-1669(96)80032-2

Fredrickson, J. K., Zachara, J. M., Kennedy, D. W., Dong, H., Onstott, T. C., Hinman, N. W., et al. (1998). Biogenic iron mineralization accompanying the dissimilatory reduction of hydrous ferric oxide by a groundwater bacterium. *Geochim. Cosmochim. Acta* 62, 3239–3257. doi: 10.1016/S0016-7037(98)00243-9

Frenzel, P., Bosse, U., and Janssen, P. H. (1999). Rice roots and methanogenesis in a paddy soil: ferric iron as an alternative electron acceptor in the rooted soil. *Soil. Biol. Biochem.* 31, 421–430. doi: 10.1016/S0038-0717(98)00144-8

Hansel, C. M., Benner, S. G., Neiss, J., Dohnalkova, A., Kukkadapu, R. K., and Fendorf, S. (2003). Secondary mineralization pathways induced by dissimilatory iron reduction of ferrihydrite under advective flow. *Geochim. Cosmochim. Acta* 67, 2977–2992. doi: 10.1016/S0016-7037(03)00276-X

Hori, T., Müller, A., Igarashi, Y., Conrad, R., and Friedrich, M. W. (2010). Identification of iron-reducing microorganisms in anoxic rice paddy soil by ^{13}C-acetate probing. *ISME J.* 4, 267–278. doi: 10.1038/ismej.2009.100

Ishii, S., Shimoyama, T., Hotta, Y., and Watanabe, K. (2008). Characterization of a filamentous biofilm community established in a cellulose-fed microbial fuel cell. *BMC Microbiol.* 8:6. doi: 10.1186/1471-2180-8-6

Jäeckel, U., and Schnell, S. (2000). Suppression of methane emission from rice paddies by ferric iron fertilization. *Soil. Biol. Biochem.* 32, 1811–1814. doi: 10.1016/S0038-0717(00)00094-8

Jiang, S., Park, S., Yoon, Y., Lee, J. H., Wu, W. M., and Phuoc, D. N. (2013). Methanogenesis facilitated by geobiochemical iron cycle in a novel syntrophic methanogenic microbial community. *Environ. Sci. Technol.* 47, 10078–10084. doi: 10.1021/es402412c

Kato, S., Hashimoto, K., and Watanabe, K. (2012). Methanogenesis facilitated by electric syntrophy via (semi) conductive iron-oxide minerals. *Environ. Microbiol.* 14, 1646–1654. doi: 10.1111/j.1462-2920.2011.02611.x

Kato, S., and Igarashi, K. (2019). Enhancement of methanogenesis by electric syntrophy with biogenic iron-sulfide minerals. *MicrobiologyOpen* 8:e00647. doi: 10.1002/mbo3.647

Kuever, J. (2014). *The Family Syntrophobacteraceae*. Berlin: Springer.

Kukkadapu, R. K., Zachara, J. M., Fredrickson, J. K., and Kennedy, D. W. (2004). Biotransformation of two-line silica-ferrihydrite by a dissimilatory Fe(III)-reducing bacterium: formation of carbonate green rust in the presence of

phosphate. *Geochim. Cosmochim. Acta* 68, 2799–2814. doi: 10.1016/j.gca.2003.12.024

Kunapuli, U., Lueders, T., and Meckenstock, R. U. (2007). The use of stable isotope probing to identify key iron-reducing microorganisms involved in anaerobic benzene degradation. *ISME J.* 1, 643–653. doi: 10.1038/ismej.2007.73

Li, H., Chang, J., Liu, P., Fu, L., Ding, D., and Lu, Y. (2015). Direct interspecies electron transfer accelerates syntrophic oxidation of butyrate in paddy soil enrichments. *Environ. Microbiol.* 17, 1533–1547. doi: 10.1111/1462-2920.12576

Li, L., Zhi, Q., Rong, J., Wang, B., Wang, Y., and Dong, Q. (2017). Excessive input of phosphorus significantly affects microbial Fe(III) reduction in flooded paddy soils by changing the abundances and community structures of *Clostridium* and *Geobacteraceae*. *Sci. Total Environ.* 60, 982–991. doi: 10.1016/j.scitotenv.2017.07.078

Liang, B., Wang, L. Y., Mbadinga, S. M., Liu, J. F., Yang, S. Z., Gu, J. D., et al. (2015). *Anaerolineaceae* and *Methanosaeta* turned to be the dominant microorganisms in alkanes-dependent methanogenic culture after long-term of incubation. *Amb. Express* 5:37. doi: 10.1186/s13568-015-0117-4

Liu, P., and Conrad, R. (2017). *Syntrophobacteraceae*-affiliated species are major propionate-degrading sulfate reducers in paddy soil. *Environ. Microbiol.* 19, 1669–1686. doi: 10.1111/1462-2920.13698

Lovley, D. R. (1987). Organic-matter mineralization with the reduction of ferric iron-a review. *Geomicrobiol. J.* 5, 375–399. doi: 10.1080/01490458709385975

Lovley, D. R. (1991). "Magnetite formation during microbial dissimilatory iron reduction," in *Iron biominerals*, eds R. B. Frankel, and R. P. Blakemore, (New York: Plenum Press), 151–166.

Lovley, D. R., and Phillips, E. J. P. (1986). Availability of ferric iron for microbial reduction in bottom sediments of the freshwater tidal Potomac River. *Appl. Environ. Microb.* 52, 751–757.

Lü, Z., and Lu, Y. (2012). *Methanocella conradii* sp. nov., a thermophilic, obligate hydrogenotrophic methanogen, isolated from Chinese rice field soil. *PLos One* 7:e35279. doi: 10.1371/journal.pone.0035279

Lueders, T., and Friedrich, M. W. (2002). Effects of amendment with ferrihydrite and gypsum on the structure and activity of methanogenic populations in rice field soil. *Appl. Environ. Microbiol.* 68, 2484–2494. doi: 10.1128/AEM.68.5.2484-2494.2002

Magoč, T., and Salzberg, S. L. (2011). FLASH: fast length adjustment of short reads to improve genome assemblies. *Bioinformatics* 27, 2957–2963. doi: 10.1093/bioinformatics/btr507

Mortimer, R. J. G., and Coleman, M. L. (1997). Microbial influence on the oxygen isotopic composition of diagenetic siderite. *Geochim. Cosmochim. Acta* 61, 1705–1711. doi: 10.1016/S0016-7037(97)00027-6

Muehe, E. M., Adaktylou, I. J., Obst, M., Zeitvogel, F., Behrens, S., Friedrich, B., et al. (2013a). Organic carbon and reducing conditions lead to cadmium immobilization by secondary Fe mineral formation in a pH-neutral soil. *Environ. Sci. Technol.* 47, 13430–13439. doi: 10.1021/es403438n

Muehe, E. M., Scheer, L., Daus, B., and Kappler, A. (2013b). Fate of arsenic during microbial reduction of biogenic versus Abiogenic As-Fe(III)-mineral coprecipitates. *Environ. Sci. Technol.* 47, 8297–8307. doi: 10.1021/es400801z

N'Guessan, A. L., Elifantz, H., Nevin, K. P., Mouser, P. J., Methé, B., Woodard, T. L., et al. (2010). Molecular analysis of phosphate limitation in *Geobacteraceae* during the bioremediation of a uranium-contaminated aquifer. *ISME J.* 4, 253–266. doi: 10.1038/ismej.2009.115

O'Loughlin, E. J., Gorski, C. A., Scherer, M. M., Boyanov, M. I., and Kemner, K. M. (2010). Effects of oxyanions, natural organic matter, and bacterial cell numbers on the bioreduction of lepidocrocite (gamma-FeOOH) and the formation of secondary mineralization products. *Environ. Sci. Technol.* 44, 4570–4576. doi: 10.1021/es100294w

Oren, A. (2014). *The Family Methanosarcinaceae*. Berlin: Springer.

Parmar, N., Gorby, Y. A., Beveridge, T. J., and Ferris, F. G. (2001). Formation of green rust and immobilization of nickel in response to bacterial reduction of hydrous ferric oxide. *Geomicrobiol. J.* 18, 375–385. doi: 10.1080/014904501753210549

Pedersen, H. D., Postma, D., and Jakobsen, R. (2006). Release of arsenic associated with the reduction and transformation of iron oxides. *Geochim. Cosmochim. Acta* 70, 4116–4129. doi: 10.1016/j.gca.2006.06.1370

Phillips, E. J. P., Lovley, D. R., and Roden, E. E. (1993). Composition of non-microbially reducible Fe^{3+} in aquatic sediments. *Appl. Environ. Microb.* 59, 2727–2729.

Qu, D., Ratering, S., and Schnell, S. (2004). Microbial reduction of weakly crystalline iron (III) oxides and suppression of methanogenesis in paddy soil. *Bull Environ. Contam. Toxicol.* 72, 1172–1181. doi: 10.1007/s00128-004-0367-3

Roden, E. E., Leonardo, M. R., and Ferris, F. G. (2002). Immobilization of strontium during iron biomineralization coupled to dissimilatory hydrous ferric oxide reduction. *Geochim. Cosmochim. Acta* 66, 2823–2839. doi: 10.1016/S0016-7037(02)00878-5

Rotaru, A. E., Shrestha, P. M., Liu, F., Nevin, K. P., and Lovley, D. R. (2014). Direct interspecies electron transfer between *Geobacter metallireducens* and *Methanosarcina barkeri* on ethanol. *Appl. Environ. Microb.* 80, 4599–4605. doi: 10.1128/AEM.00895-14

Rui, J., Qiu, Q., and Lu, Y. (2011). Syntrophic acetate oxidation under thermophilic methanogenic condition in chinese paddy field soil. *FEMS Microbiol. Ecol.* 77, 264–273. doi: 10.1111/j.1574-6941.2011.01104.x

Sakai, S., Conrad, R., Liesack, W., and Imachi, H. (2010). *Methanocella arvoryzae* sp. nov., a hydrogenotrophic methanogen isolated from rice field soil. *Int. J. Syst. Evol. Micr.* 60, 2918–2923. doi: 10.1099/ijs.0.020883-0

Sakai, S., Imachi, H., Hanada, S., Ohashi, A., Harada, H., and Kamagata, Y. (2008). *Methanocella paludicola* gen. nov., sp. nov., a methane-producing archaeon, the first isolate of the lineage "Rice Cluster I," and proposal of the new archaeal order Methanocellales ord. nov. *Int. J. Syst. Evol. Micr.* 58, 929–936. doi: 10.1099/ijs.0.65571-0

Schwertmann, U., and Cornell, R. M. (2000). *Iron Oxides in the Laboratory: Preparation and Characterization.* New York, NY: Wiley-VCH.

Sekiguchi, Y., Takahashi, H., Kamagata, Y., Ohashi, A., and Harada, H. (2001). In situ detection, isolation, and physiological properties of a thin filamentous microorganism abundant in methanogenic granular sludges: a novel isolate affiliated with a clone cluster, the green non-sulfur bacteria, subdivision I. *Appl. Environ. Microb.* 67, 5740–5749. doi: 10.1128/AEM.67.12.5740-5749.2001

Sobieraj, M., and Boone, D. R. (2006). "*Syntrophomonadaceae*," in *The Prokaryotes*, eds M. Dworkin, S. Falkow, E. Rosenberg, K. H. Schleifer, and E. Stackebrandt, (New York, NY: Springer), 1041–1049.

Tang, J., Zhuang, L., Ma, J., Tang, Z., Yu, Z., and Zhou, S. (2016). Secondary mineralization of ferrihydrite affects microbial methanogenesis in Geobacter-Methanosarcina cocultures. *Appl. Environ. Microb.* 82, 5869–5877. doi: 10.1128/AEM.01517-16

Tebo, B. M., and Obraztsova, A. Y. (1998). Sulfate-reducing bacterium grows with Cr(VI), U(VI), Mn(IV), and Fe(III) as electron acceptors. *FEMS Microbiol. Lett.* 162, 193–198. doi: 10.1111/j.1574-6968.1998.tb12998.x

Tufano, K. J., Benner, S. G., Mayer, K. U., Marcus, M. A., Nico, P. S., and Fendorf, S. (2009). Aggregate-scale heterogeneity in iron (hydr)oxide reductive transformations. *Vadose Zone J.* 8, 1004–1012. doi: 10.2136/vzj2008.0090

Viggi, C. C., Rossetti, S., Fazi, S., Paiano, P., Majone, M., and Aulenta, F. (2014). Magnetite particles triggering a faster and more robust syntrophic pathway of methanogenic propionate degradation. *Environ. Sci. Technol.* 48, 7536–7543. doi: 10.1021/es5016789

Yamada, C., Kato, S., Ueno, Y., Ishii, M., and Igarashi, Y. (2015). Conductive iron oxides accelerate thermophilic methanogenesis from acetate and propionate. *J. Biosci. Bioeng.* 119, 678–682. doi: 10.1016/j.jbiosc.2014.11.001

Yamada, T., Sekiguchi, Y., Imachi, H., Kamagata, Y., Ohashi, A., and Harada, H. (2005). Diversity, localization, and physiological properties of filamentous microbes belonging to Chloroflexisubphylum I in mesophilic and thermophilic methanogenic sludge granules. *Appl. Environ. Microbiol.* 71, 7493–7503. doi: 10.1128/AEM.71.11.7493-7503.2005

Yi, W. J., You, J. H., Zhu, C., Wang, B. L., and Qu, D. (2013). Diversity, dynamic and abundance of *Geobacteraceae* species in paddy soil following slurry incubation. *Eur. J. Soil Biol.* 56, 11–18. doi: 10.1016/j.ejsobi.2013.01.004

Zachara, J. M., Kukkadapu, R. K., Fredrickson, J. K., Gorby, Y. A., and Smith, S. C. (2002). Biomineralization of poorly crystalline fe(III) Oxides by Dissimilatory Metal Reducing Bacteria (DMRB). *Geomicrobiol. J.* 19, 179–207.

Zheng, S., Wang, B., Liu, F., and Wang, O. (2017). Magnetite production and transformation in the methanogenic consortia from coastal riverine sediments. *J. Microbiol.* 55, 862–870. doi: 10.1007/s12275-017-7104-1

Zhuang, L., Tang, J., Wang, Y., Hu, M., and Zhou, S. (2015a). Conductive iron oxide minerals accelerate syntrophic cooperation in methanogenic benzoate degradation. *J. Hazard. Mater.* 293, 37–45. doi: 10.1016/j.jhazmat.2015.03.039

Zhuang, L., Xu, J. L., Tang, J., and Zhou, S. G. (2015b). Effect of ferrihydrite biomineralization on methanogenesis in an anaerobic incubation from paddy soil. *J. Geophys. Res-Biogeo.* 120, 876–886. doi: 10.1002/2014JG002893